

---

# CONSISTNAV: CLOSING THE ACTION CONSISTENCY GAP IN ZERO-SHOT OBJECT NAVIGATION WITH SEMANTIC EXECUTIVE CONTROL

**Haosen Wang\***  
Sun Yat-sen University

**Zhenyang Li\***  
The University of Hong Kong

**Yinqiang Zhang**  
The University of Hong Kong

**Zongqi He**  
The University of Hong Kong

**Lutao Jiang**  
Hong Kong University of  
Science and Technology  
(Guangzhou)

**Kai Li**  
City University of Hong Kong

**Yizhou Zhao**  
Carnegie Mellon University

**Liaoyuan Fan**  
The University of Hong Kong

**Wenjian Hou**  
Sun Yat-sen University

**Tingbang Liang**  
Sun Yat-sen University

**Yibin Wen**  
Sun Yat-sen University

**Defeng Gu†**  
Sun Yat-sen University

\*Equal contribution. †Corresponding author.

## ABSTRACT

Zero-shot object navigation has advanced rapidly with open-vocabulary detectors, image–text models, and language-guided exploration. However, even after current methods detect a plausible target hypothesis, the agent may still oscillate between exploration and pursuit, or abandon the object near success. We identify this failure mode as an action consistency gap: semantic evidence is repeatedly reinterpreted at each step without persistent commitment across the episode. We introduce ConsistNav, a training-free zero-shot ObjectNav framework built around a semantic executive composed of three coordinated modules: Finite-State Executive Controller stages target pursuit through guarded semantic phases; Persistent Candidate Memory accumulates cross-frame target evidence into stable object hypotheses; and Stability-Aware Action Control suppresses rotational stagnation, ineffective pursuit, and unverified stopping. This design changes neither the detector nor the low-level planner; instead, it controls when semantic evidence should influence navigation and when it should be suppressed or revisited. We conduct extensive experiments on HM3D and MP3D, where ConsistNav achieves state-of-the-art results among compared zero-shot ObjectNav methods and improves SR by 11.4% and SPL by 7.9% over the controlled baseline on MP3D. Ablation studies and real-world deployment experiments further demonstrate the effectiveness and robustness of the proposed executive mechanism.

## 1 INTRODUCTION

Object-goal navigation requires an embodied agent to find a target-category instance in an unseen environment and stop within the success radius (Batra et al., 2020). In zero-shot ObjectNav (ZSON), open-vocabulary detectors, vision–language models, and language-guided frontier exploration have improved semantic search without task-specific policy training (Radford et al., 2021; Khandelwal et al., 2022; Majumdar et al., 2022; Yu et al., 2023; Zhou et al., 2023; Yin et al., 2024; Yokoyama et al., 2024; Zhang et al., 2025). However, many modular systems still optimize *semantic evidence production* or *frontier scoring* more directly than the conversion of evidence

---

into sustained action (Yamauchi, 1997; Zhou et al., 2023; Yin et al., 2024; Yokoyama et al., 2024; Zhang et al., 2025). When semantic observations are repeatedly reinterpreted against newly scored frontiers, an agent may oscillate between exploration and pursuit, abandon a plausible target near success, or stop from an insufficiently verified viewpoint. We call this the *action consistency gap*: useful evidence is observed, but the induced objective, commitment, and stop decision are not preserved through approach, verification, and termination.

We introduce ConsistNav, a training-free perception–planning–execution framework for ZSON centered on a semantic executive. The executive contains three coordinated modules. *Finite-State Executive Controller* stages target pursuit through guarded semantic phases. *Persistent Candidate Memory* accumulates cross-frame target evidence into stable object hypotheses. *Stability-Aware Action Control* suppresses rotational stagnation, ineffective pursuit, and unverified stopping. Together, these modules convert open-vocabulary semantic evidence into temporally consistent action while leaving the detector, semantic mapper, and low-level planner unchanged.

We evaluate ConsistNav through controlled experiments under the same underlying stack, isolating the effect of executive control from changes in perception or planning capacity. Beyond standard Success Rate (SR) and Success weighted by Path Length (SPL), we analyze diagnostic failure categories that separate verified success from infeasible targets, unstable commitments, frontier exhaustion, timeouts, and missed targets. We further report real-world quantitative deployment results, showing that the same executive principles transfer beyond simulation.

Our contributions are threefold:

- **Evidence-to-action diagnosis.** We formulate the *action consistency gap* in ZSON, showing that retained semantic evidence can still produce unstable pursuit, weak verification, and premature stopping when commitment is not preserved through execution.
- **Executive semantic commitment.** We introduce a training-free semantic executive that combines persistent candidate memory, guarded finite-state control, and stability-aware action filtering to turn open-vocabulary evidence into stable, recoverable, and termination-aware navigation commitments.
- **Same-stack validation.** With the detector, mapper, frontier planner, and low-level planner fixed, ConsistNav achieves state-of-the-art results among compared ZSON methods, with ablations, failure diagnostics, and real-world deployment showing that the gains come from executive control rather than a stronger perception or planning backbone.

## 2 RELATED WORK

### 2.1 SEMANTIC FRONTIER NAVIGATION

Zero-shot ObjectNav increasingly relies on pretrained visual–language representations rather than category-specific navigation policies. CLIP-style goal embeddings and open-vocabulary detections enable navigation to unseen categories (Khandelwal et al., 2022; Majumdar et al., 2022), while later systems add frontier maps, language priors, scene graphs, and multimodal commonsense reasoning (Gadre et al., 2023; Yokoyama et al., 2024; Yu et al., 2023; Shah et al., 2022; Zhou et al., 2023; Yin et al., 2024; Rajvanshi et al., 2024; Zhang et al., 2025). Representative semantic frontier methods combine occupancy mapping, frontier scoring, and semantic fusion to decide *where* evidence should guide exploration. Compared with ApexNav’s target-centric fusion (Zhang et al., 2025), ConsistNav studies *when* accumulated evidence should become a commitment and how it should be verified, suppressed, or recovered during action.

### 2.2 CLASSICAL EXECUTIVE CONTROL FOR ZSON

Our work is also connected to classical planning and temporal abstraction, where persistent goals, pre-conditions, recovery behaviors, and action hierarchies provide explicit structure for long-horizon decision making (Ghallab et al., 2004; LaValle, 2006; Sutton et al., 1999; Kaelbling et al., 1998). Similar ideas appear in local navigation, behavior trees, frontier exploration, and modular semantic mapping, which separate mapping, planning, and action while exposing guard conditions for when a controller should continue, recover, or switch modes (Fox et al., 1997; Colledanchise & Ögren, 2018;

Yamauchi, 1997; Chaplot et al., 2020a; Chaplot et al., 2020b). We do not claim finite-state control as new; instead, our novelty lies in identifying belief-to-action inconsistency in open-vocabulary semantic navigation, defining measurable failure modes, and showing that a lightweight executive can close this gap within a modern VLM-based ObjectNav stack. Thus, ConsistNav is not a generic state machine, but an executive layer specialized for failures that emerge when semantic evidence, frontier exploration, and stop decisions interact online.

### 2.3 PERCEPTION-EXPLORATION-CONTROL STRUCTURE FOR ZSON

Recent embodied pipelines commonly organize ZSON into a modular perception–exploration–control loop, using open-vocabulary detectors, vision–language models, and promptable segmenters to obtain object evidence (Liu et al., 2024; Li et al., 2022; Minderer et al., 2022; Gu et al., 2022; Li et al., 2023; Kirillov et al., 2023; Zhang et al., 2023) while relying on frontier exploration, semantic mapping, and geometric planning for navigation. In these systems, perception proposes object evidence, mapping stores it in spatial context, and planning converts the current map into frontier or target-directed motion (Yamauchi, 1997; Fox et al., 1997; Mur-Artal et al., 2015; Campos et al., 2021; McCormac et al., 2017; Rosinol et al., 2020). These components improve perception and search, but they do not specify how semantic evidence should be committed, recovered, or rejected during execution, especially when detections are intermittent or viewpoints are ambiguous. The execution layer still needs a policy for when to trust a weak cue, when to keep approaching it, and when to return to exploration after contradictory observations. Learning-based ObjectNav, hierarchical policies, options, and POMDP formulations can learn or model such couplings under supervision or large-scale training (Wijmans et al., 2020; Chaplot et al., 2020a; Chaplot et al., 2020b; Ramakrishnan et al., 2022; Ramrakhya et al., 2022; Yadav et al., 2023; Ramrakhya et al., 2023; Sutton et al., 1999; Kaelbling et al., 1998). ConsistNav instead targets the zero-shot setting, enforcing a lightweight reliability contract between perception and planning without retraining detector–planner-specific policies.

## 3 METHOD

### 3.1 PROBLEM FORMULATION

We study ObjectNav in previously unseen indoor scenes, where an embodied agent must find an instance of a target category from egocentric RGB-D observations and start-relative odometry. The agent outputs discrete actions under a fixed budget and is evaluated by SR and SPL. Our goal is to improve evidence-to-action consistency while keeping perception and low-level planning fixed.

### 3.2 OVERVIEW

ConsistNav is a perception–planning–execution framework for zero-shot ObjectNav. As shown in Figure 1, open-vocabulary perception projects scored RGB-D evidence into semantic maps; the executive maintains persistent candidates and a finite-state controller; and the planner executes the selected frontier-conditioned or candidate-conditioned subgoal.

At step  $t$ , the agent receives target category  $g$ , RGB-D observation  $o_t = (I_t, D_t)$ , and pose estimate  $\mathbf{x}_t = (p_t, \theta_t)$ . Perception and mapping fuse scored target/non-target observations into a persistent candidate memory

$$\mathcal{C}_t = \{c_1^{(t)}, \dots, c_{N_t}^{(t)}\}. \quad (1)$$

Each candidate stores location, confidence, semantic evidence, consistency, ITM history, and recovery flags. Conditioned on this memory, pose, progress, and failed subgoals, ConsistNav maintains a semantic control state

$$q_t \in \{\text{SEARCH, SUSPECT, APPROACH, VERIFY, FINAL-APPROACH, FAILOVER, SUCCESS}\} \quad (2)$$

that gates semantic evidence before geometric planning. Given  $q_t$ , ConsistNav selects a frontier, approach, verification, docking, or recovery subgoal. Stability-aware action control then suppresses spin, detects stalls, bounds recovery, and authorizes STOP only under verified multi-cue evidence. The action output is

$$a_t \in \mathcal{A} = \{\text{FORWARD, LEFT, RIGHT, STOP}\}. \quad (3)$$

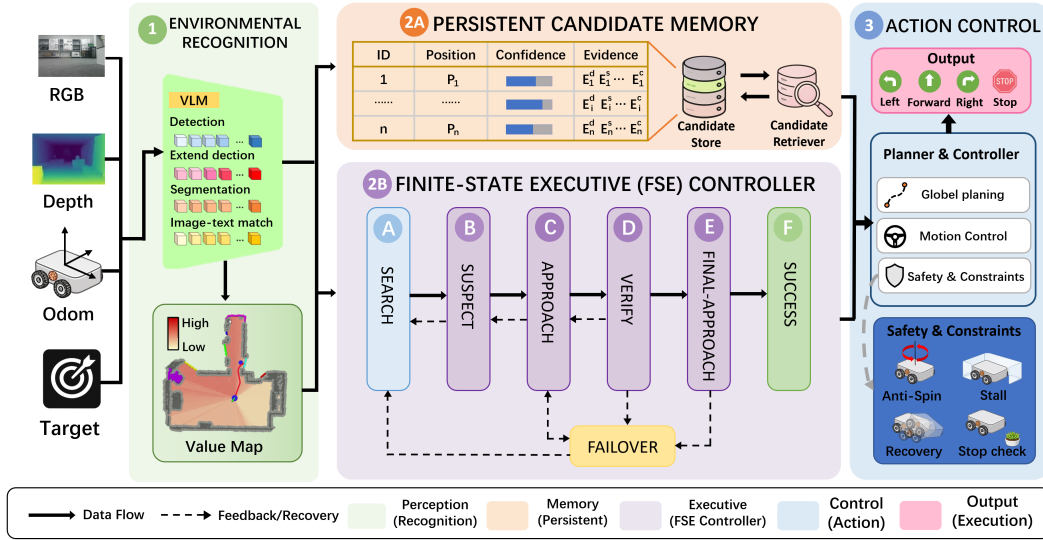


Figure 1: **ConsistNav pipeline.** ① Perception converts RGB-D and target cues through VLM scoring into value maps; ②A ②B planning maintains candidates and selects frontier/candidate subgoals; ③ execution outputs LEFT, FORWARD, RIGHT, and STOP actions through the FSE controller.

Thus,  $\mathcal{C}_t$  stores accumulated evidence,  $q_t$  gates planning, and  $a_t$  remains in the standard ObjectNav action space.

The following subsections make these components concrete. Section 3.3 details candidate memory, Section 3.4 explains the Finite-State Executive Controller, and Section 3.5 describes stability-aware action control.

### 3.3 PERSISTENT CANDIDATE MEMORY

As shown in Fig. 2 (left), persistent candidate memory builds a semantic candidate map and stores hypotheses by confidence, high (0.7–1.0), medium (0.4–0.7), or low (0–0.4), with last-update time. It aggregates evidence, suppression signals, and recovery status into a ranked candidate set for commitment and control.

**Candidate representation.** Each object hypothesis is represented as

$$c_i^{(t)} = \left( \mu_i^{(t)}, \hat{c}_i^{(t)}, n_i^{(t)}, m_{i,+}^{(t)}, m_{i,-}^{(t)}, s_i^{(t)}, \bar{r}_i^{(t)}, f_i^{(t)}, u_i^{(t)} \right). \quad (4)$$

where  $\mu_i^{(t)} \in \mathbb{R}^2$  is the candidate position,  $\hat{c}_i^{(t)}$  and  $n_i^{(t)}$  are accumulated positive and negative evidence,  $m_{i,+}^{(t)}$  and  $m_{i,-}^{(t)}$  count target and non-target observations,  $s_i^{(t)}$  is a consistency score,  $\bar{r}_i^{(t)}$  stores ITM history, and  $f_i^{(t)}, u_i^{(t)}$  encode failure, cooldown, and later recovery status.

**Association and belief update.** Given a projected semantic observation  $\tilde{\mu}_t$ , the executive associates it with the nearest candidate and merges it when the distance is below the merge radius  $r_m$ .

For a matched candidate, the center is updated by exponential smoothing,

$$\mu_{i^*}^{(t+1)} = (1 - \lambda)\mu_{i^*}^{(t)} + \lambda\tilde{\mu}_t, \quad (5)$$

where  $\lambda \in (0, 1)$  controls the contribution of the new observation; we use  $\lambda = 0.3$ .

Confidence and negative evidence are updated asymmetrically:

$$\hat{c}_i^{(t+1)} = \min(1, \hat{c}_i^{(t)} + \alpha y_t - 0.12\alpha(1 - y_t)), \quad n_i^{(t+1)} = n_i^{(t)} + \beta z_t. \quad (6)$$

Here,  $y_t$  indicates target consistency,  $z_t$  indicates verify-stage failure, and  $\alpha, \beta$  control confidence gain and failure penalty. This asymmetric update lets target evidence raise confidence quickly while allowing non-target or failed evidence to suppress candidates gradually.

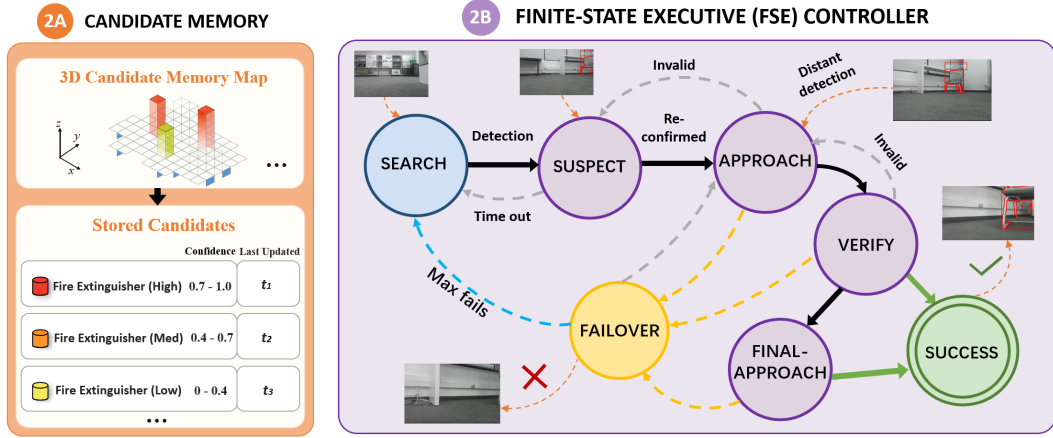


Figure 2: **Candidate Memory and FSE Controller.** Left: Candidate Memory builds/stores the semantic candidate map. Right: seven-state FSE transitions, with black/green for commitment/success, gray/yellow for invalidation/recovery, and blue for returning to search.

**Consistency score and priority.** To decide which hypotheses can influence control, the executive first converts the memory fields into a consistency score

$$s_i^{(t)} = \text{clip}_{[0,1]} \left( w_c \hat{c}_i^{(t)} + w_r \frac{m_{i,+}^{(t)}}{m_{i,+}^{(t)} + m_{i,-}^{(t)} + \varepsilon} + w_o \min(1, m_{i,+}^{(t)}/6) + w_l \bar{l}_i^{(t)} - w_f \phi_i^{(t)} \right), \quad (7)$$

where  $\varepsilon > 0$  prevents division by zero,  $\phi_i^{(t)}$  summarizes failure-related penalties, and  $w_c, w_r, w_o, w_l, w_f$  are fixed executive weights.

Candidate selection then ranks hypotheses by combining confidence, negative evidence, consistency, repeated support, and ITM confirmation, while penalizing stale, failed, or recently visited candidates.

Overall, this memory turns noisy semantic observations into a compact ranked candidate set for the executive controller.

### 3.4 FINITE-STATE EXECUTIVE CONTROLLER

As shown in Fig. 2 (right), the FSE Controller provides the executive flow that converts persistent candidates into committed, verified, and recoverable navigation behavior. We describe this process through the *Commitment state space*, *Guarded commitment chain*, and *Failure loop* below.

**Commitment state space.** ConsistNav uses the semantic state space defined in Sec. 3.2. These states monotonically raise commitment from frontier search to candidate holding, pursuit, close-range verification, final docking, recovery, and terminal stop, while keeping recovery as an explicit route for invalidated hypotheses.

**Guarded commitment chain.** The nominal chain raises commitment from open-ended search to verified termination while preserving a single active intent:

$$\text{SEARCH} \rightarrow \text{SUSPECT} \rightarrow \text{APPROACH} \rightarrow \text{VERIFY} \rightarrow \text{FINAL-APPROACH} \rightarrow \text{SUCCESS}. \quad (8)$$

but every edge is guarded by candidate viability, rank persistence, distance, and verification evidence. A candidate is viable only if

$$\mathcal{V}_t = \{i : f_i^{(t)} = 0, t \geq u_i^{(t)}, m_{i,+}^{(t)} > m_{i,-}^{(t)}, \hat{c}_i^{(t)} \geq \tau_c, s_i^{(t)} \geq \tau_{\text{cons}}\}, \quad (9)$$

where  $f_i$  marks failed hypotheses,  $u_i$  is the cooldown step,  $m_{i,+}, m_{i,-}$  count target and non-target support, and  $\hat{c}_i, s_i$  denote confidence and consistency. Viable candidates are ranked by  $\pi_i^{(t)}$ , which combines confidence, consistency, repeated support, ITM evidence, and stale/failure penalties. The

executive enters SUSPECT only for a strong or persistent top candidate, advances after re-confirmation or stable rank, and switches from APPROACH to VERIFY when

$$d(p_t, \mu_{i^*}^{(t)}) \leq r_v + \mathbb{I}[k_{\text{app}} \geq N_{\text{verify}}] r_{\text{extra}}, \quad (10)$$

or when approach progress saturates. Verification succeeds only under a bounded semantic-geometric gate:

$$h_t \geq 2, \quad d_t^{\text{best}} \leq r_{\text{stop}}, \quad \kappa_t \geq \tau_{\text{conf}}, \quad m_{i,+}^{(t)} \geq M_{\text{obs}}, \quad m_{i,+}^{(t)} > m_{i,-}^{(t)}, \quad \bar{\eta}_t \geq \tau_{\text{itm}} \quad (11)$$

so  $\text{STOP}$  requires agreement among target hits, geometry, confidence, observation count, and ITM evidence.

**Failure loop.** Complementary to semantic escalation, ConsistNav defines a recovery route for commitments that should be weakened rather than blindly continued:

$$\mathcal{Q}_{\text{commit}} \rightarrow \text{FAILOVER} \rightarrow \mathcal{Q}_{\text{return}}. \quad (12)$$

The committed and returnable state sets are

$$\begin{cases} \mathcal{Q}_{\text{commit}} = \{\text{SUSPECT}, \text{APPROACH}, \text{VERIFY}, \text{FINAL-APPROACH}\}, \\ \mathcal{Q}_{\text{return}} = \{\text{SEARCH}, \text{APPROACH}, \text{VERIFY}\}. \end{cases} \quad (13)$$

It then either completes docking for a recently verified close candidate, switches to the best unfrozen candidate, or returns to frontier search when no viable candidate or failover budget remains.

Overall, ConsistNav converts open-vocabulary semantic evidence into stable navigation commitment. It avoids over-trusting single-frame detections while also preventing brief occlusions or missed detections from prematurely discarding a plausible target.

### 3.5 STABILITY-AWARE ACTION CONTROL

Stability-Aware Action Control makes planner commands state-conditioned, so the same planner follows different executive intents. In SEARCH, ConsistNav follows frontier exploration; in APPROACH and FINAL-APPROACH, it selects a candidate-conditioned subgoal:

$$\gamma_t^* = \arg \min_{\gamma \in \mathcal{G}_t} \left[ d(\gamma, \mu_{i^*}^{(t)}) + \lambda_v \mathbb{I}[\gamma \in \mathcal{R}_t] + \lambda_f \mathbb{I}[\gamma \in \mathcal{F}_t] \right], \quad (14)$$

where  $d(\gamma, \mu_{i^*}^{(t)})$  is the planner distance to the active candidate,  $\mathcal{R}_t$  and  $\mathcal{F}_t$  denote visited and failed regions, and  $\lambda_v, \lambda_f$  weight the corresponding penalties. The objective preserves candidate commitment while discouraging repeated or failed subgoals; four guards then stabilize execution.

**Anti-spin control.** Let  $\Delta p_t = \|p_t - p_{t-1}\|$  and  $\Delta \theta_t = |\theta_t - \theta_{t-1}|$ . The executive maintains a spin budget  $b_t^{\text{spin}}$  that increases when  $\Delta \theta_t > 0$  but  $\Delta p_t < \delta_{\text{move}}$ , resets after sufficient translation, and suppresses additional pure turns once  $b_t^{\text{spin}} > B_{\text{spin}}$  by requiring the current or resampled subgoal to satisfy a minimum translation margin.

**Stall detection.** The controller uses a stall counter  $s_t$  for physical progress and a best-distance tracker  $d_t^{\text{best}} = \min_{\tau \leq t} d(p_\tau, \mu_{i^*})$  for semantic pursuit. If  $\Delta p_t < \delta_{\text{move}}$  or  $d_t^{\text{best}}$  fails to improve by margin  $\epsilon_d$  for  $K_s$  steps in committed states, the guard triggers verification, recovery, or failover according to candidate strength and proximity.

**Bounded recovery.** Recovery is finite and updates memory. Failed pursuit increases the active candidate’s negative evidence  $n_i^-$  and failure count  $f_i$ , decays its confidence/consistency, and records the region in  $\mathcal{F}_t$ . If no progress is observed within the  $B_r$ -step escape budget, FAILOVER switches candidate, refreshes the docking point, returns to search, or falls back to frontier exploration.

**Verified stop check.** ConsistNav authorizes STOP only through a semantic-geometric gate that aggregates target hits  $h_t$ , best distance  $d_t^{\text{best}}$ , maximum confidence  $\kappa_t$ , and average ITM score  $\eta_t^{\text{ITM}}$ . The gate requires target evidence to dominate non-target evidence; unexpected STOP outputs outside SUCCESS are intercepted as recovery or heading reset.

Together, these guards make the action layer explicit: rotation is bounded by  $b_t^{\text{spin}}$ , pursuit by  $d_t^{\text{best}}$ , recovery by  $(n_i^-, f_i, B_r)$ , and termination by  $(h_t, d_t^{\text{best}}, \kappa_t, \eta_t^{\text{ITM}})$ .

---

## 4 EXPERIMENTS

We describe the benchmarks and implementation used for controlled evaluation, compare with prior ObjectNav methods, analyze failure modes, validate executive components through ablations, and report real-world deployment results.

### 4.1 BENCHMARKS AND IMPLEMENTATION DETAILS

**Datasets.** We evaluate under the Habitat ObjectNav protocol (Savva et al., 2019; Batra et al., 2020) on three benchmark settings: MP3D (Chang et al., 2017), HM3Dv1 (Ramakrishnan et al., 2021), and HM3Dv2. HM3Dv1 uses the HM3D-Semantics-v0.1 validation split with 2000 episodes over 20 scenes and 6 goal categories; HM3Dv2 uses the v0.2 validation split with 1000 episodes over 36 scenes and the same categories; MP3D uses 2195 validation episodes over 11 Matterport3D scenes and 21 categories. Together, these benchmarks test transfer across scene scale, reconstruction source, and category distribution.

**Evaluation metrics.** We report SR and SPL, the two standard metrics for ObjectNav (Anderson et al., 2018). SR measures the fraction of episodes in which the agent reaches the target and issues a valid stop, while SPL further discounts successful episodes by path inefficiency. Let  $s_i$  denote success,  $l_i$  the executed path length, and  $l_i^*$  the shortest feasible path length for episode  $i$ ; higher values indicate better performance for both metrics. The metrics are defined as follows:

$$SR = \frac{1}{N} \sum_{i=1}^N s_i, \quad SPL = \frac{1}{N} \sum_{i=1}^N s_i \frac{l_i^*}{\max(l_i, l_i^*)}. \quad (15)$$

**Implementation details.** All methods follow the same Habitat protocol with a  $[0, 5]$  m sensing range, 0.2 m success radius, and 0.88 m RGB-D camera height. To isolate executive control, all variants use the same perception–mapping–planning stack with YOLO-World/GroundingDINO, MobileSAM, and BLIP-2. We fix all executive thresholds across datasets, including  $\tau_c = 0.15$ ,  $\tau_{\text{cons}} = 0.42$ ,  $r_v = 0.8$  m,  $r_{\text{stop}} = 0.28$  m,  $\tau_{\text{conf}} = 0.30$ , and  $\tau_{\text{itm}} = 0.12$ . The internal  $r_{\text{stop}}$  gate only triggers candidate-centered stop verification; success still requires the Habitat evaluator’s 0.2 m valid-STOP criterion.

### 4.2 COMPARISON WITH STATE-OF-THE-ART

Table 1 compares ConsistNav with representative ObjectNav methods on HM3Dv2, HM3Dv1, and MP3D. Prior rows are literature-reported contextual baselines; the primary evidence is a deterministic same-stack comparison against the Non-executive baseline, which keeps the detector, mapper, planner, simulator protocol, episode list, and action budget fixed. Under this setting, ConsistNav improves SR/SPL by +8.0%/ +3.2% on HM3Dv2, +3.6%/ +1.8% on HM3Dv1, and +11.4%/ +7.9% on MP3D. Among the methods listed in Table 1, it obtains the strongest reported results on all three benchmarks, indicating that persistent memory, finite-state commitment, verified stopping, and bounded failover improve reliability without changing the underlying stack.

### 4.3 FAILURE CAUSE ANALYSIS

We assign each episode to one outcome after inspecting the trajectory, semantic detections, stop decision, and target passage. As shown in Fig. 4, we use six categories: (1) *Success*, reaching and verifying the target; (2) *Infeasible / Different Floor*, unreachable or topologically separated targets; (3) *Unstable Commitment*, observed evidence followed by abandonment or unreliable stopping; (4) *Frontier Exhaustion*, no remaining frontier goals; (5) *Step-limit Timeout*, search or recovery exceeding the action budget; and (6) *Missing Target*, passing the target without verification.

Figure 4 compares ConsistNav with the Non-executive method and shows that the executive shifts controllable failures toward verified success. On HM3Dv2 and MP3D, success rises by +8.00% and +11.34% while timeout drops by 3.00% and 10.21%, indicating that memory, guarded commitment, and verified stopping sustain promising pursuits and reduce missed or premature termination. MP3D frontier exhaustion increases from 4.92% to 10.52%, reflecting a conservative trade-off: weak

Table 1: ObjectNav results on HM3Dv2, HM3Dv1, and MP3D. Prior rows are literature-reported contextual baselines; controlled same-stack comparisons are described in the text and ablations.

Method	Unsupervised	Zero-shot	HM3Dv2		HM3Dv1		MP3D	
			SR	SPL	SR	SPL	SR	SPL
PONI (Ramakrishnan et al., 2022)	No	No	–	–	–	–	31.8	12.1
ProcTHOR (Deitke et al., 2022)	No	No	–	–	54.4	31.8	–	–
ZSON (Majumdar et al., 2022)	Yes	No	–	–	25.5	12.6	15.3	4.8
ProcTHOR-ZS (Deitke et al., 2022)	Yes	No	–	–	13.2	7.7	–	–
OpenFMNav (Kuang et al., 2024)	Yes	Yes	–	–	54.9	24.4	37.2	15.7
InstructNav (Long et al., 2024)	Yes	Yes	58.0	20.9	–	–	–	–
VLFM (Yokoyama et al., 2024)	Yes	Yes	63.6	32.5	52.5	30.4	36.4	17.5
TriHelper (Zhang et al., 2024)	Yes	Yes	–	–	56.5	25.3	–	–
SG-Nav (Yin et al., 2024)	Yes	Yes	49.6	25.5	54.0	24.9	<u>40.2</u>	16.0
ApexNav (Zhang et al., 2025)	Yes	Yes	<u>76.2</u>	<u>38.0</u>	<u>59.6</u>	<u>33.0</u>	39.2	<u>17.8</u>
<b>ConsistNav (ours)</b>	Yes	Yes	<b>84.2</b>	<b>41.2</b>	<b>63.2</b>	<b>34.8</b>	<b>50.6</b>	<b>25.7</b>

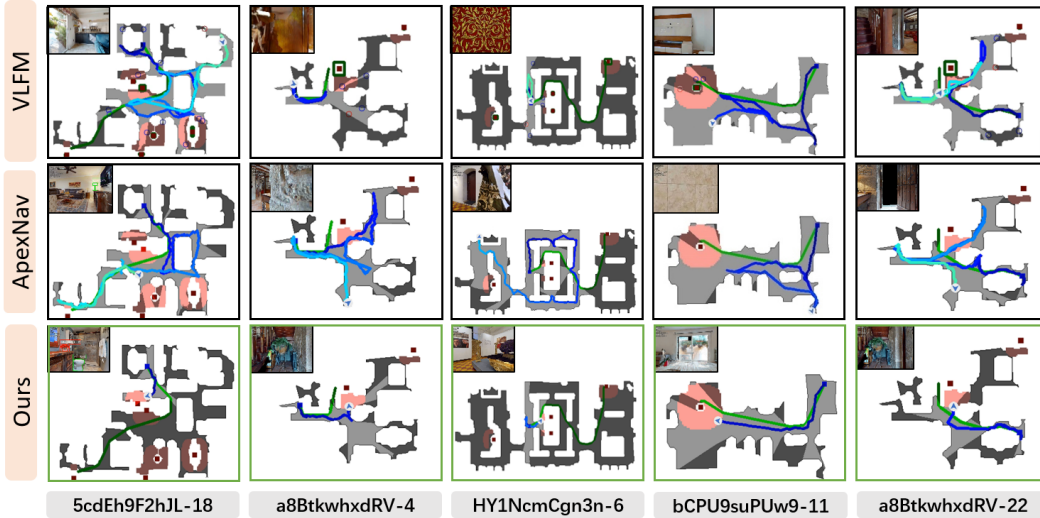


Figure 3: **Simulation results on HM3Dv2.** Qualitative comparison of ConsistNav, VLFM, and ApexNav. Each column shows one episode; green/blue paths denote reference/agent trajectories, and green/black frames denote success/failure.

candidates become explicit search failures rather than unstable commitments, while infeasible and late-discovery cases remain dataset-level limits.

#### 4.4 ABLATION STUDY

**Ablation analysis.** Table 2 shows progressive improvement as the three executive components are added, indicating that ConsistNav benefits from the interaction between memory, executive control, and action stabilization rather than a single heuristic. The monotonic trend also suggests that each module removes a different bottleneck: noisy semantic evidence, unstable commitment, and low-level action inconsistency. This staged comparison is therefore more diagnostic than a single full-system comparison, because it separates whether gains come from remembering candidates, deciding when

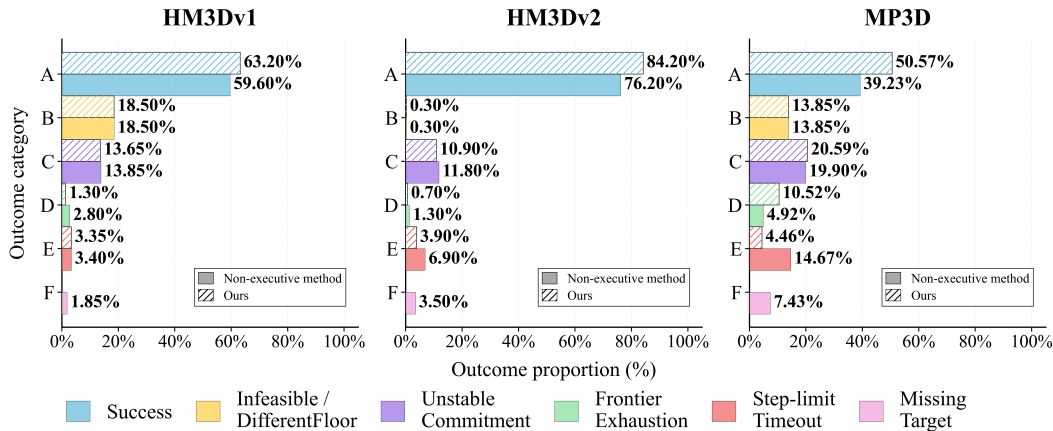


Figure 4: **Failure-cause comparison.** Outcome statistics for the Non-executive method and **ConsistNav** on HM3Dv1, HM3Dv2, and MP3D, covering verified success and five residual failure modes.

Table 2: Executive ablation on HM3Dv2 under the same underlying stack. PCM, FSEC, and SAAC denote persistent candidate memory, Finite-State Executive Controller, and stability-aware action control.

Variant	PCM	FSEC	SAAC	SR	SPL
Non-executive baseline	✗	✗	✗	76.20	38.00
+ Persistent Candidate Memory	✓	✗	✗	77.10	39.60
+ Finite-State Executive Controller	✓	✓	✗	81.00	40.75
+ Stability-Aware Action Control	✓	✓	✓	<b>84.20</b>	<b>41.24</b>

Table 3: Real-world deployment results with 10 physical trials per target.

Target	Episodes	Success	Time(avg)
Chair	10	100	157s
Plant	10	100	140s
Couch	10	100	164s
TV	10	100	160s
Overall	40	100	155s

to pursue them, or executing the pursuit robustly. **(a) Persistent Candidate Memory.** PCM provides the first gain of +0.90% SR and +1.60% SPL by stabilizing cross-frame evidence and suppressing transient detections, although memory alone cannot decide when to commit, recover, or stop. **(b) Finite-State Executive Controller.** FSEC contributes the largest improvement, adding +3.90% SR and +1.15% SPL, showing that guarded state transitions are the main mechanism for turning stored candidates into reliable commitments. **(c) Stability-Aware Action Control.** SAAC further improves SR by +3.20% and SPL by +0.49% by handling spin, stall, verified stopping, and failover after target selection. Overall, the full executive achieves +8.00% SR and +3.24% SPL over the Non-executive baseline, confirming that the three modules address complementary stages of the evidence-to-action pipeline.

#### 4.5 REAL-WORLD DEPLOYMENT

We deploy ConsistNav on an AgileX LIMO robot and run inference on an NVIDIA RTX 4090 workstation. Figure 5 provides qualitative real-world comparisons with a Non-executive baseline, showing representative navigation behaviors under real sensing and control latency. Table 3 reports the physical-scene evaluation: 40 tasks are conducted in a  $10 \times 10 \text{ m}^2$  office scene and a  $30 \times 10 \text{ m}^2$  constructed home scene across chair, plant, couch, and TV targets, validating the robustness of the deployed system.

## 5 CONCLUSION

We presented ConsistNav, a training-free semantic executive that achieves state-of-the-art zero-shot ObjectNav performance without relying on online large language models. ConsistNav closes the action consistency gap by combining persistent candidate memory, the Finite-State Executive Controller, verified stopping, and bounded failover, while keeping the perception, mapping, frontier planning, and local control stack fixed. Across HM3D and MP3D, it improves both goal acquisition

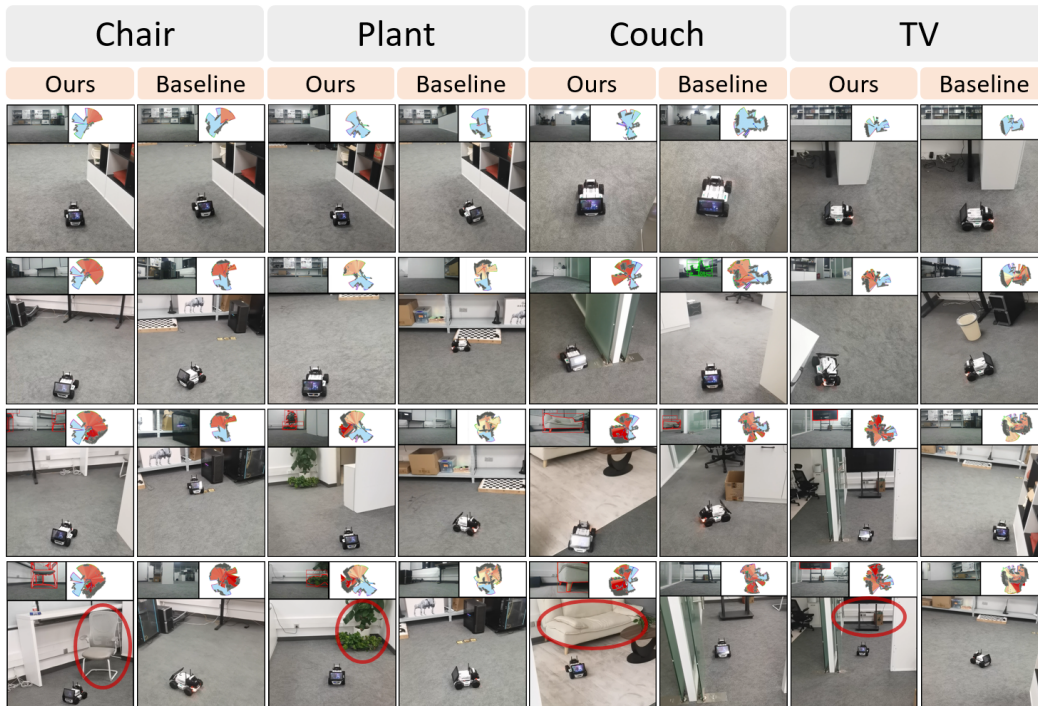


Figure 5: **Real-world deployment comparison.** Visual comparison of the Non-executive baseline and ConsistNav on four target tasks using the AgileX LIMO platform. The results illustrate that ConsistNav maintains target hypotheses, verifies close-range evidence, and stops reliably under real sensor and timing conditions.

and path efficiency, and ablations show that each executive component contributes complementary gains. These results highlight explicit executive structure as a decisive ingredient for robust open-vocabulary navigation and a practical path toward deployable embodied agents.

**Limitations.** Real-world inference currently runs on a remote PC rather than fully onboard the robot. The results also depend on coordination between the simulator, planner, and verified-stop interface, reflecting the sensitivity of ObjectNav benchmarks to execution-level design.

**Future work.** Future work will study adaptive transition thresholds while preserving the explicit executive structure, and extend ConsistNav to multi-target or instruction-conditioned navigation where commitment must reason over competing semantic goals.

## REFERENCES

- Peter Anderson, Angel Chang, Devendra Singh Chaplot, Alexey Dosovitskiy, Saurabh Gupta, Vladlen Koltun, Jana Kosecka, Jitendra Malik, Roozbeh Mottaghi, Manolis Savva, and Amir R. Zamir. On evaluation of embodied navigation agents. *arXiv preprint arXiv:1807.06757*, 2018.
- Dhruv Batra, Aaron Gokaslan, Aniruddha Kembhavi, Oleksandr Maksymets, Roozbeh Mottaghi, Manolis Savva, Alexander Toshev, and Erik Wijmans. ObjectNav revisited: On evaluation of embodied agents navigating to objects. *arXiv preprint arXiv:2006.13171*, 2020.
- Carlos Campos, Richard Elvira, Juan J. Gómez Rodríguez, José M. M. Montiel, and Juan D. Tardós. ORB-SLAM3: An accurate open-source library for visual, visual-inertial, and multimap SLAM. *IEEE Transactions on Robotics*, 37(6):1874–1890, 2021.
- Angel X. Chang, Angela Dai, Thomas Funkhouser, Maciej Halber, Matthias Niessner, Manolis Savva, Shuran Song, Andy Zeng, and Yinda Zhang. Matterport3d: Learning from RGB-D data in indoor environments. In *Proceedings of the International Conference on 3D Vision (3DV)*, 2017.

- 
- Devendra Singh Chaplot, Dhiraj Gandhi, Abhinav Gupta, and Ruslan Salakhutdinov. Object goal navigation using goal-oriented semantic exploration. In *Advances in Neural Information Processing Systems (NeurIPS)*, 2020a.
- Devendra Singh Chaplot, Dhiraj Gandhi, Saurabh Gupta, Abhinav Gupta, and Ruslan Salakhutdinov. Learning to explore using active neural SLAM. In *International Conference on Learning Representations (ICLR)*, 2020b.
- Michele Colledanchise and Petter Ögren. *Behavior Trees in Robotics and AI: An Introduction*. CRC Press, 2018.
- Matt Deitke, Eli VanderBilt, Alvaro Herrasti, Luca Weihs, Kiana Ehsani, Jordi Salvador, Winson Han, Eric Kolve, Aniruddha Kembhavi, and Roozbeh Mottaghi. ProcTHOR: Large-scale embodied AI using procedural generation. In *Advances in Neural Information Processing Systems (NeurIPS)*, 2022.
- Dieter Fox, Wolfram Burgard, and Sebastian Thrun. The dynamic window approach to collision avoidance. *IEEE Robotics & Automation Magazine*, 4(1):23–33, 1997.
- Samir Yitzhak Gadre, Mitchell Wortsman, Gabriel Ilharco, Ludwig Schmidt, and Shuran Song. COWS on PASTURE: Baselines and benchmarks for language-driven zero-shot object navigation. In *Proceedings of the IEEE/CVF Conference on Computer Vision and Pattern Recognition (CVPR)*, 2023.
- Malik Ghallab, Dana Nau, and Paolo Traverso. *Automated Planning: Theory and Practice*. Elsevier, 2004.
- Xiuye Gu, Tsung-Yi Lin, Weicheng Kuo, and Yin Cui. Open-vocabulary object detection via vision and language knowledge distillation. In *International Conference on Learning Representations (ICLR)*, 2022.
- Leslie Pack Kaelbling, Michael L. Littman, and Anthony R. Cassandra. Planning and acting in partially observable stochastic domains. *Artificial Intelligence*, 101(1–2):99–134, 1998.
- Apoorv Khandelwal, Luca Weihs, Roozbeh Mottaghi, and Aniruddha Kembhavi. Simple but effective: CLIP embeddings for embodied AI. In *Proceedings of the IEEE/CVF Conference on Computer Vision and Pattern Recognition (CVPR)*, 2022.
- Alexander Kirillov, Eric Mintun, Nikhila Ravi, Hanzi Mao, Chloe Rolland, Laura Gustafson, Tete Xiao, Spencer Whitehead, Alexander C. Berg, Wan-Yen Lo, Piotr Dollár, and Ross Girshick. Segment anything. In *Proceedings of the IEEE/CVF International Conference on Computer Vision (ICCV)*, 2023.
- Yuxuan Kuang, Hai Lin, and Meng Jiang. OpenFMNav: Towards open-set zero-shot object navigation via vision-language foundation models. In *Findings of the Association for Computational Linguistics: NAACL 2024*, pp. 338–351, 2024.
- Steven M. LaValle. *Planning Algorithms*. Cambridge University Press, 2006.
- Junnan Li, Dongxu Li, Silvio Savarese, and Steven Hoi. BLIP-2: Bootstrapping language-image pre-training with frozen image encoders and large language models. In *Proceedings of the International Conference on Machine Learning (ICML)*, 2023.
- Liunian Harold Li, Pengchuan Zhang, Haotian Zhang, Jianwei Yang, Chunyuan Li, Yiwu Zhong, Lijuan Wang, Lu Yuan, Lei Zhang, Jenq-Neng Hwang, Kai-Wei Chang, and Jianfeng Gao. Grounded language-image pre-training. In *Proceedings of the IEEE/CVF Conference on Computer Vision and Pattern Recognition (CVPR)*, 2022.
- Shilong Liu, Zhaoyang Zeng, Tianhe Ren, Feng Li, Hao Zhang, Jie Yang, Qing Jiang, Chunyuan Li, Jianwei Yang, Hang Su, Jun Zhu, and Lei Zhang. Grounding DINO: Marrying DINO with grounded pre-training for open-set object detection. In *Proceedings of the European Conference on Computer Vision (ECCV)*, 2024.

- 
- Yuxing Long, Wenzhe Cai, Hongcheng Wang, Guanqi Zhan, and Hao Dong. InstructNav: Zero-shot system for generic instruction navigation in unexplored environment. *arXiv preprint arXiv:2406.04882*, 2024.
- Arjun Majumdar, Gunjan Aggarwal, Bhavika Devnani, Judy Hoffman, and Dhruv Batra. ZSON: Zero-shot object-goal navigation using multimodal goal embeddings. In *Advances in Neural Information Processing Systems (NeurIPS)*, 2022.
- John McCormac, Ankur Handa, Andrew J. Davison, and Stefan Leutenegger. SemanticFusion: Dense 3D semantic mapping with convolutional neural networks. In *Proceedings of the IEEE International Conference on Robotics and Automation (ICRA)*, 2017.
- Matthias Minderer, Alexey Gritsenko, Austin Stone, Maxim Neumann, Dirk Weissenborn, Alexey Dosovitskiy, Aravindh Mahendran, Anurag Arnab, Mostafa Dehghani, Zhuoran Shen, Xiao Wang, Xiaohua Zhai, Thomas Kipf, and Neil Houlsby. Simple open-vocabulary object detection with vision transformers. In *Proceedings of the European Conference on Computer Vision (ECCV)*, 2022.
- Raul Mur-Artal, J. M. M. Montiel, and Juan D. Tardós. ORB-SLAM: A versatile and accurate monocular SLAM system. *IEEE Transactions on Robotics*, 31(5):1147–1163, 2015.
- Alec Radford, Jong Wook Kim, Chris Hallacy, Aditya Ramesh, Gabriel Goh, Sandhini Agarwal, Girish Sastry, Amanda Askell, Pamela Mishkin, Jack Clark, Gretchen Krueger, and Ilya Sutskever. Learning transferable visual models from natural language supervision. In *Proceedings of the International Conference on Machine Learning (ICML)*, 2021.
- Abhinav Rajvanshi, Karan Sikka, Xiao Lin, Boram Lee, Han-Pang Chiu, and Alvaro Velasquez. SayNav: Grounding large language models for dynamic planning to navigation in new environments. In *Proceedings of the International Conference on Automated Planning and Scheduling (ICAPS)*, 2024.
- Santhosh K. Ramakrishnan, Devendra Singh Chaplot, Ziad Al-Halah, Jitendra Malik, and Kristen Grauman. PONI: Potential functions for ObjectGoal navigation with interaction-free learning. In *Proceedings of the IEEE/CVF Conference on Computer Vision and Pattern Recognition (CVPR)*, 2022.
- Santhosh Kumar Ramakrishnan, Aaron Gokaslan, Erik Wijmans, Oleksandr Maksymets, Alexander Clegg, John M. Turner, Eric Undersander, Wojciech Galuba, Andrew Westbury, Angel X. Chang, Manolis Savva, Yili Zhao, and Dhruv Batra. Habitat-Matterport 3D Dataset (HM3D): 1000 large-scale 3d environments for embodied AI. In *Proceedings of the Neural Information Processing Systems Track on Datasets and Benchmarks (NeurIPS Datasets)*, 2021.
- Ram Ramrakhya, Eric Undersander, Dhruv Batra, and Abhishek Das. Habitat-web: Learning embodied object-search strategies from human demonstrations at scale. In *Proceedings of the IEEE/CVF Conference on Computer Vision and Pattern Recognition (CVPR)*, 2022.
- Ram Ramrakhya, Dhruv Batra, Erik Wijmans, and Abhishek Das. PIRLNav: Pretraining with imitation and RL finetuning for ObjectNav. In *Proceedings of the IEEE/CVF Conference on Computer Vision and Pattern Recognition (CVPR)*, 2023.
- Antoni Rosinol, Marcus Abate, Yun Chang, and Luca Carlone. Kimera: An open-source library for real-time metric-semantic localization and mapping. In *Proceedings of the IEEE International Conference on Robotics and Automation (ICRA)*, 2020.
- Manolis Savva, Abhishek Kadian, Oleksandr Maksymets, Yili Zhao, Erik Wijmans, Bhavana Jain, Julian Straub, Jia Liu, Vladlen Koltun, Jitendra Malik, Devi Parikh, and Dhruv Batra. Habitat: A platform for embodied AI research. In *Proceedings of the IEEE/CVF International Conference on Computer Vision (ICCV)*, 2019.
- Dhruv Shah, Błażej Osipiński, Brian Ichter, and Sergey Levine. LM-Nav: Robotic navigation with large pretrained models of language, vision, and action. In *Proceedings of the Conference on Robot Learning (CoRL)*, 2022.

- 
- Richard S. Sutton, Doina Precup, and Satinder Singh. Between MDPs and semi-MDPs: A framework for temporal abstraction in reinforcement learning. *Artificial Intelligence*, 112(1–2):181–211, 1999.
- Erik Wijmans, Abhishek Kadian, Ari Morcos, Stefan Lee, Irfan Essa, Devi Parikh, Manolis Savva, and Dhruv Batra. DD-PPO: Learning near-perfect PointGoal navigators from 2.5 billion frames. In *International Conference on Learning Representations (ICLR)*, 2020.
- Karmesh Yadav, Ram Ramrakhya, Arjun Majumdar, Naoki Yokoyama, Alexei Baevski, Zsolt Kira, Oleksandr Maksymets, and Dhruv Batra. OVRL-V2: A simple state-of-art baseline for ImageNav and ObjectNav. *arXiv preprint arXiv:2303.07798*, 2023.
- Brian Yamauchi. A frontier-based approach for autonomous exploration. In *Proceedings of the IEEE International Symposium on Computational Intelligence in Robotics and Automation (CIRA)*, 1997.
- Hang Yin, Xiuwei Xu, Zhenyu Wu, Jie Zhou, and Jiwen Lu. SG-Nav: Online 3d scene graph prompting for llm-based zero-shot object navigation. In *Advances in Neural Information Processing Systems (NeurIPS)*, 2024.
- Naoki Yokoyama, Sehoon Ha, Dhruv Batra, Jiuguang Wang, and Bernadette Bucher. VLFM: Vision-language frontier maps for zero-shot semantic navigation. In *Proceedings of the IEEE International Conference on Robotics and Automation (ICRA)*, 2024.
- Banguo Yu, Hamidreza Kasaei, and Ming Cao. L3MVN: Leveraging large language models for visual target navigation. In *Proceedings of the IEEE/RSJ International Conference on Intelligent Robots and Systems (IROS)*, 2023.
- Chaoning Zhang, Dongshen Han, Yu Qiao, Jung Uk Kim, Sung-Ho Bae, Seungkyu Lee, and Choong Seon Hong. Faster segment anything: Towards lightweight SAM for mobile applications. *arXiv preprint arXiv:2306.14289*, 2023.
- Lingfeng Zhang, Qiang Zhang, Hao Wang, Erjia Xiao, Zixuan Jiang, Honglei Chen, and Renjing Xu. TriHelper: Zero-shot object navigation with dynamic assistance. In *Proceedings of the IEEE/RSJ International Conference on Intelligent Robots and Systems (IROS)*, 2024.
- Mingjie Zhang, Yuheng Du, Chengkai Wu, Jinni Zhou, Zhenchao Qi, Jun Ma, and Boyu Zhou. ApexNav: An adaptive exploration strategy for zero-shot object navigation with target-centric semantic fusion. *IEEE Robotics and Automation Letters*, 2025.
- Kaiwen Zhou, Kaizhi Zheng, Connor Pryor, Yilin Shen, Hongxia Jin, Lise Getoor, and Xin Eric Wang. ESC: Exploration with soft commonsense constraints for zero-shot object navigation. In *Proceedings of the International Conference on Machine Learning (ICML)*, 2023.